Appl. Phys. B 68, 1143–1146 (1999) / DOI 10.1007/s003409900066

Applied Physics B
Lasers
and Optics

Rapid communication

Type-I non-critically phase-matched second-harmonic generation in $Gd_{1-x}Y_xCa_4O(BO_3)_3$

P.B.W. Burmester[1], **T. Kellner**[1], **K. Petermann**[1], **G. Huber**[1], **R. Uecker**[2], **P. Reiche**[2]

[1] Institut für Laser-Physik, Universität Hamburg, Jungiusstr. 9a, 20355 Hamburg
(Fax: +49-40/42838-6281, E-mail: burmester@physnet.uni-hamburg.de)
[2] Institut für Kristallzüchtung, Rudower Chaussee 6, Geb. 19.30, 12489 Berlin
(Fax: +49-30/6392-3003)

Received: 19 April 1999/Published online: 5 May 1999

Abstract. Second-harmonic generation was z-cut observed $Gd_{1-x}Y_xCa_4O(BO_3)_3$ ($Gd_{1-x}Y_x$COB) and the dependence of the phase-matching wavelength on the mixing ratio x has been investigated. The dependence on both temperature and angle tuning was examined as well. We found the suitable composition for noncritical frequency doubling at 930 nm, which is the lasing wavelength of Nd:$YAlO_3$ on the $^4F_{3/2} \rightarrow {}^4I_{9/2}$ transition.

PACS: 42.25.Lc; 42.65.Ky; 42.70.Mp

Recently, interest in the new nonlinear materials of the $ReCa_4O(BO_3)_3$ family (Re = rare earth) has grown. In comparison to the conventional and established nonlinear materials, ReCOB combines some advantageous properties. As well as its good nonlinear optical properties, i.e. high nonlinear coefficients and transparency in the UV [1], it has good mechanical properties, allowing easy polishing. Furthermore, these materials have a high damage threshold and are non-hygroscopic. They melt nearly congruently and big crystals can be grown. The existence of large lattice sites offers the possibility of rare earth ion doping, and good lasing properties are already proved. This even makes ReCOB appropriate for self-frequency doubling.

Frequency doubling of Nd-doped ground-state lasers with wavelengths between 900 nm and 950 nm into the blue spectral region can be realized in GdCOB and YCOB by type-I critical phase matching. The orientation of the crystal (θ, φ) that meets the phase-matching condition has to be calculated from the Sellmeier equations. Accordingly, critical phase-matching can be achieved in GdCOB at these wavelengths with the wave vector $\boldsymbol{k}$ orientated either in the xy plane or in the zy plane of the indicatrix [2]. However, it is experimentally observed that "there is a lack of second-harmonic generation in the zy plane" [3]. In YCOB second-harmonic generation can be realized in this spectral range with crystals cut in the xy or zx plane [3]. The disadvantage of critical phase matching is the low angular acceptance and the presence of beam walk-off between the fundamental and the second harmonic.

In contrast, non-critical phase matching, which can be achieved by cutting the crystal along one of the main dielectrical axes, x, y or z, yields large angular acceptance bandwidths. One further advantage of non-critical phase matching is the lack of beam walk-off, so that the crystal can be very long in order to raise the efficiency of the frequency conversion.

In z-cut crystals, phase matching can be realized with the polarization of the fundamental and the second harmonic parallel to the y and x axes, respectively. In [1] the pure materials YCOB and GdCOB are investigated and Sellmeier coefficients are given. According to [1] the theoretical phase-matching wavelengths for z-cut YCOB and GdCOB are 840 nm and 966 nm, respectively. In [3] slightly different Sellmeier coefficients for YCOB are given. As a result, the phase-matching wavelength is calculated to be 827 nm. M. Yoshimura et al. [4] suggested growing $Gd_{1-x}Y_x$COB and tuning the non-critical phase-matching wavelength in the range from 827 nm to 966 nm by changing the compositional parameter x.

In the case of z-cut crystals, the output power of the second-harmonic is proportional to the square of the nonlinear coefficient d_{12}. Unfortunately this is the smallest of the nonlinear coefficients in YCOB ($d_{12} = 0.43\,\mathrm{pm\,V^{-1}}$) and in GdCOB ($d_{12} = 0.24\,\mathrm{pm\,V^{-1}}$) as well [3]. Indeed, there is no possibility to use x-cut or y-cut $Gd_{1-x}Y_x$COB as a type-I second-harmonic generator for neodymium ground-state lasers. Using the Sellmeier coefficients determined by M. Iwai et al. [1] one expects to tune the non-critical phase-matching wavelength in x-cut crystals from 1486 nm (YCOB) to 1633 nm (GdCOB); y-cut $Gd_{1-x}Y_x$COB seems to be interesting for non-critical second-harmonic generation into the UV. The range for phase matching extends from 735 nm (YCOB) to 838 nm (GdCOB). Also, y-cut $Gd_{0.275}Y_{0.725}$COB was reported for type-II phase matching at 1.06 μm [5].

We have grown $Gd_{1-x}Y_x$COB of different compositions with the aim of second-harmonic generation in the spectral region of neodymium ground-state lasers. We found that z-cut $Gd_{0.84}Y_{0.16}$COB converts the infrared radiation of Nd:$YAlO_3$ emitted from the $^4F_{3/2} \rightarrow {}^4I_{9/2}$ transition (930 nm) into blue light (465 nm) by non-critical type-I phase-matching.

1 Crystal growth of (Gd,Y)COB

The crystals have been grown using the Czochralski technique with radio-frequency induction heating [2]. The pulling process is automized by the crucible weighing method. Because the melting temperatures of the mixed crystals lie between those of the GdCOB (1480 °C) [2] and YCOB (1510 °C) [6], an iridium crucible (40 ml) was used. The power of additional windings of the RF coil was coupled to a cylindrical afterheater. Both the crucible and the afterheater were embedded in alumina ceramics. This resulted in the axial temperature gradient above the melt surface being so flat that no remarkable thermal stress remained in the grown crystal. The crystal growth was performed in flowing nitrogen atmosphere. The growth rate was $2\,\mathrm{mm\,h^{-1}}$ and the rotation $10\,\mathrm{min^{-1}}$. The starting materials Gd_2O_3, Y_2O_3, $CaCO_3$, and B_2O_3 were of 5N and 4N quality. They were dried, mixed, and sintered following standard procedures. The melting behaviour of GdCOB and YCOB is reported to be congruent and nearly congruent, respectively [2, 6]. Therefore we mixed the (Gd,Y)COB corresponding to the aimed composition of the crystal. According to microprobe analysis (ems, camebax), the actual yttrium concentration is slightly higher than the concentration ratio of the starting powders. The average segregation coefficient for yttrium was found to be 1.12. Because the phase-matching experiments were performed in z-orientated rods, the crystals were grown perpendicular to the (801) plane, which is close to the z axis of the indicatrix. The crystal boules reached 65 mm in length and 18 mm in diameter and the yield was about 40%. Their habit was cylindrical without any facet.

2 Phase-matching measurements

2.1 Angle tuning

In Fig. 1 the dependence of the phase-matching wavelength λ_{pm} on the mixing parameter x is shown. The collimated beam from a Ti:sapphire laser with 600 mW output power was focussed ($f = 40$ mm) into crystals with different mixing ratios. The phase-matching wavelengths were determined by tuning the wavelength of the Ti:sapphire for maximum blue output power. The wavelengths were measured with a 1-m spectrometer.

The crystal containing 16% yttrium is appropriate for frequency doubling of Nd:$YAlO_3$ lasing on the ground-state transition at 930 nm. This crystal is approximately 15 mm long and the phase-matching condition proved to be quite insensitive to variation of the angle θ between the $\boldsymbol{k}$ vector of the incident Ti:sapphire beam and the z axis. In Fig. 2 the phase matching-wavelength is shown as a function of the angle of the propagating beam to the z axis inside the crystal. The external angles are even larger since the refractive index is roughly 1.7. The saddle point in Fig. 2, which is characterised by $\partial\lambda_{pm}/\partial\theta = 0$, corresponds to the case $\boldsymbol{k} \parallel \boldsymbol{z}$. In this adjustment the phase-matching wavelength of $Gd_{0.84}Y_{0.16}$COB was determined to be $\lambda_{pm} = 929.3$ nm at room temperature.

Adjusting the angles $\theta_{zx} \neq 0°$ in the zx plane increases the phase-matching wavelength, while angles $\theta_{zy} \neq 0°$ in the zy plane yield shorter wavelengths. To check the observed wavelength tuning behaviour, calculations using the Sellmeier coefficients of pure GdCOB [1] were carried out. For angle tuning in both planes, the calculated wavelength dependence on angle tuning for GdCOB is compared with the measured dependence for $Gd_{0.84}Y_{0.16}$COB. In Fig. 3a,b the solid line (right-hand scale) shows the calculated dependence of the phase-matching wavelength on angle tuning for pure GdCOB. The left-hand scale refers to the measured wavelenghts of $Gd_{0.84}Y_{0.16}$COB. Because of the difference in composition, the absolute values of the phase-matched wavelengths differ by almost 40 nm and therefore the scales were shifted against each other. Indeed, the measured wavelength dependence on angle tuning agrees well with the calculated one. As predicted by the theory for GdCOB,

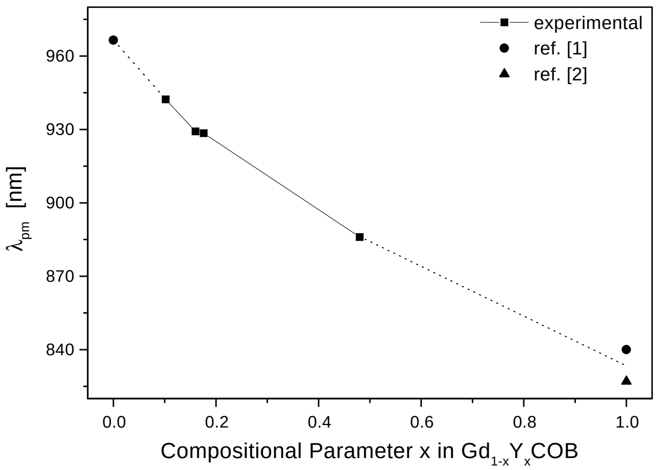

Fig. 1. Phase-matching wavelengths of z-cut $Gd_{1-x}Y_x$COB against the compositional parameter x

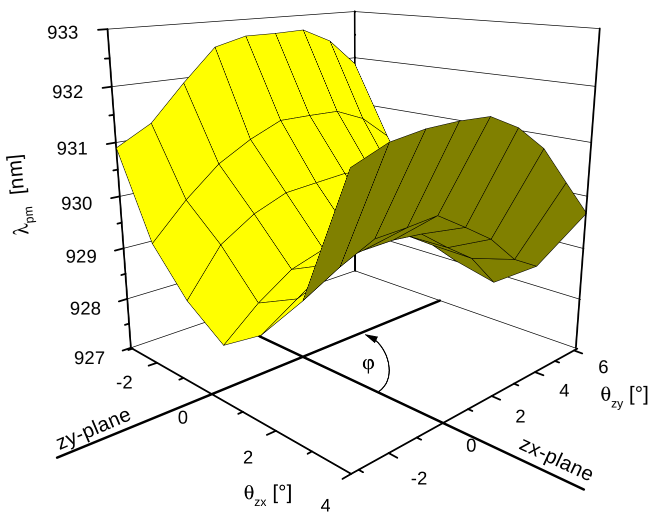

Fig. 2. Phase-matching wavelength as a function of angle tuning

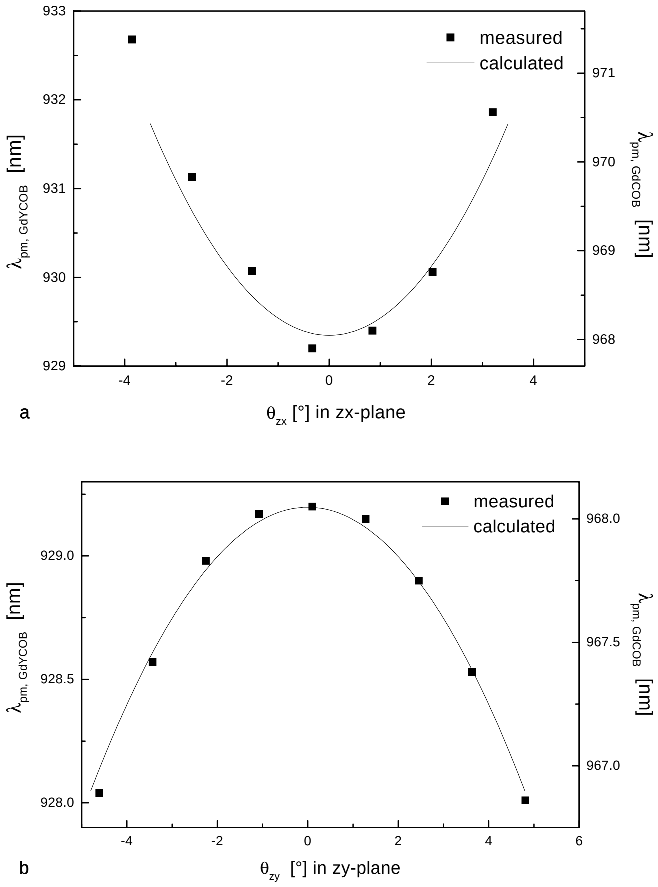

Fig. 3a,b. Calculated phase matching of GdCOB (*right scale*) and measured phase matching of $Gd_{0.84}Y_{0.16}COB$ (*left scale*) for variation of θ in the zx and zy planes

the measured variation of the phase-matching wavelength is stronger for angle tuning in the zx plane than for tuning in the zy plane.

The angular acceptance bandwidth is defined by the FWHM of the $\text{sinc}^2(\Delta kl/2)$ function, which is proportional to the power of the second-harmonic. The corresponding Δk_{FWHM} is given by

$$\Delta k_{\text{FWHM}} = \frac{1.772\pi}{l} \tag{1}$$

The dependence of Δk on θ can be expressed as a series of powers:

$$\Delta k \approx \Delta k(0) + \left.\frac{\partial \Delta k}{\partial \theta}\right|_{\Delta k=0} \Delta\theta + \left.\frac{\partial^2 \Delta k}{\partial \theta^2}\right|_{\Delta k=0} \Delta\theta^2 + \ldots . \tag{2}$$

Since we are dealing with non-critical phase matching, the second derivative is the first non-vanishing term. With $\Delta k = \Delta n 4\pi/\lambda$ and $\Delta n = n_y(\lambda) - n_x(\lambda/2)$ the angular acceptance bandwidth is obtained by combining (1) and (2):

$$\sqrt{l\Delta\theta^2} = \left[\frac{1.772\lambda}{4(\partial\Delta n/\partial\lambda)(\partial^2\lambda/\partial\theta^2)}\right]^{1/2} . \tag{3}$$

$\partial^2\lambda/\partial\theta^2$ was obtained from a fit (harmonic approximation) to the experimental data shown in Fig. 3a,b. To determine $\partial\Delta n/\partial\lambda$ for $Gd_{0.84}Y_{0.16}COB$ we calculated the values for GdCOB and YCOB using the Sellmeier equations [1] and weighing them with the composition ratio. Thus for angle tuning in the zx and zy planes, the values for the internal angular acceptance bandwidths $l^{1/2}\Delta\theta$ are 29.7 $\text{cm}^{1/2}$ mrad and 62.1 $\text{cm}^{1/2}$ mrad, respectively.

2.2 Temperature tuning

The influence of the temperature on the phase-matching condition was also examined. For this, the crystal was positioned in an oven. The ***k*** vector of the Ti:sapphire radiation was parallel to the z axis. The temperature was increased gradually from 20 °C up to 140 °C in steps of 10 °C. After temperature equilibrium was reached, the wavelength of the Ti:sapphire laser was tuned in such a way that the intensity of the generated blue light was maximum. In the same way, the phase-matching wavelengths were also measured while decreasing the temperature. Comparing the two measurements, we detected neither hysteresis nor any other anomaly. In Fig. 4 the phase-matching wavelengths, averaged from the readings at increasing and decreasing temperature, are drawn versus the temperature. It is found that there is only little variation of the phase-matching wavelength with the temperature. The correlation is linear in the temperature range from 20 °C to 140 °C and $\mathrm{d}\lambda_{\text{pm}}/\mathrm{d}T$ was determined to be 0.016 nm/K.

With considerations analogue to those for the angular acceptance bandwidth, one obtains the temperature acceptance bandwidth. However, since the first derivative $\mathrm{d}\lambda_{\text{pm}}/\mathrm{d}T$ does not vanish, the corresponding expression is

$$l\Delta T = \frac{1.772\lambda}{4(\partial\Delta n/\partial\lambda)(\partial\lambda/\partial T)} . \tag{4}$$

According to this calculation, the value of the temperature acceptance bandwidth $l\Delta T$ for $Gd_{0.84}Y_{0.16}COB$ is 42.8 cm K which is 5.5 times that of LBO. This is in good agreement with the values for the pure materials GdCOB ($l\Delta T = 38$ cm K) and YCOB ($l\Delta T = 65$ cm K) [1].

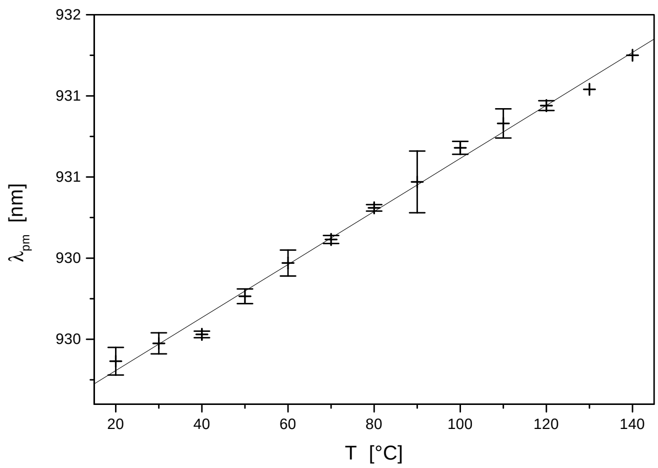

Fig. 4. Phase-matching wavelength vs. temperature

3 Summary

We have presented z-cut $Gd_{0.84}Y_{0.16}COB$ as a type-I non-critically phase-matched second-harmonic generator for 930-nm light. This composition is appropriate for frequency conversion of a Nd:$YAlO_3$ laser on the ground-state transition. Laser experiments are now in progress.

The dependence of the phase-matching wavelength on angle tuning was examined in the zx and zy planes. The internal angle acceptance bandwidths $l^{1/2}\Delta\theta$ were determined to be 29.7 $cm^{1/2}$ mrad and 62.1 $cm^{1/2}$ mrad, respectively.

Temperature tuning was also investigated. The phase-matching wavelength is proportional to the temperature at least in the temperature range from 20 °C to 140 °C. The temperature acceptance bandwidth $l\Delta T$ is 42.8 cm K.

The large acceptance bandwidths, the possibility of growing big crystals by the Czochralski technique and the high non-linearity, coupled with the possibility of active ion doping for self-frequency-doubling, make $Gd_{1-x}Y_xCOB$ a good candidate for commercial applications.

Acknowledgements. We would like to thank Mrs B. Cornelisen, Mineralogisch-Petrographisches Institut, Universität Hamburg, for the microprobe analysis.

References

1. M. Iwai, T. Kobayashi, H. Furuya, Y. Mori, T. Sasaki: Jpn. J. Appl. Phys. **36**(2), 3a (1997)
2. G. Aka, A. Kahn-Harari, F. Mougel, D. Vivien, F. Salin, P. Coquelin, P. Colin, D. Pelenc, J. Damelet: J. Opt. Soc. Am. B **14**, 9 (1997)
3. F. Mougel, G. Aka, F. Salin, D. Pelenc, A. Kahn-Harari, D. Vivien: Conference on Advanced Solid State Lasers, Technical Digest, paper WB11 (1999)
4. M. Yoshimura, T. Kobayashi, H. Furuya, Y. Mori, T. Sasaki: Conference on Lasers and Electro-Optics, Technical Digest, paper CWG2 (1998)
5. M. Yoshimura, H. Furuya, I. Yamada, K. Murase, H. Nakao, M. Yamazaki, Y. Mori, T. Sasaki: Conference on Advanced Solid State Lasers, Technical Digest, postdeadline paper pd11 (1999)
6. Q. Ye, B.H.T. Chai: J. Crystal Growth **197**, 1 (1999)